




Cardiac remodelling in a baboon model of intrauterine growth restriction mimics accelerated ageing

Anderson H. Kuo¹ , Cun Li², Jinqi Li³, Hillary F. Huber² , Peter W. Nathanielsz^{2,4} and Geoffrey D. Clarke^{1,3,4} 

¹Department of Radiology, University of Texas Health Science Center at San Antonio, San Antonio, TX, USA

²Department of Animal Science, University of Wyoming, Laramie, WY, USA

³Research Imaging Institute, University of Texas Health Science Center at San Antonio, San Antonio, TX, USA

⁴Southwest National Primate Center, San Antonio, TX, USA

Key points

- Rodent models of intrauterine growth restriction (IUGR) successfully identify mechanisms that can lead to short-term and long-term detrimental cardiomyopathies but differences between rodent and human cardiac physiology and placental-fetal development indicate a need for models in precocial species for translation to human development.
- We developed a baboon model for IUGR studies using a moderate 30% global calorie restriction of pregnant mothers and used cardiac magnetic resonance imaging to evaluate offspring heart function in early adulthood.
- Impaired diastolic and systolic cardiac function was observed in IUGR offspring with differences between male and female subjects, compared to their respective controls.
- Aspects of cardiac impairment found in the IUGR offspring were similar to those found in normal controls in a geriatric cohort.
- Understanding early cardiac biomarkers of IUGR using non-invasive imaging in this susceptible population, especially taking into account sexual dimorphisms, will aid recognition of the clinical presentation, development of biomarkers suitable for use in humans and management of treatment strategies.

Abstract Extensive rodent studies have shown that reduced perinatal nutrition programmes chronic cardiovascular disease. To enable translation to humans, we developed baboon offspring cohorts from mothers fed *ad libitum* (control) or 70% of the control *ad libitum* diet in pregnancy and lactation, which were growth restricted at birth. We hypothesized that intrauterine growth restriction (IUGR) offspring hearts would show impaired function and a premature ageing phenotype. We studied IUGR baboons (8 male, 8 female, 5.7 years), control offspring (8 male, 8 female, 5.6 years – human equivalent approximately 25 years), and normal elderly (OLD) baboons (6 male, 6 female, mean 15.9 years). Left ventricular (LV) morphology and systolic and diastolic function were evaluated with cardiac MRI and normalized to body surface area. Two-way ANOVA by group and sex (with $P < 0.05$) indicated ejection fraction, 3D sphericity indices, cardiac index, normalized systolic volume, normalized LV wall thickness, and average filling rate differed by group. Group and sex differences were found for normalized LV wall thickening and normalized myocardial mass, without interactions. Normalized peak LV filling rate and diastolic sphericity index were not correlated in control but strongly correlated in OLD and IUGR baboons. IUGR programming in baboons produces myocardial remodelling, reduces systolic and diastolic function, and results in the emergence of a premature ageing phenotype in the heart. To our knowledge, this is the first demonstration of the specific characteristics of cardiac programming and early life functional decline with ageing in an IUGR non-human primate model. Further studies across the life span will determine progression of cardiac dysfunction.

(Received 8 June 2016; accepted after revision 15 October 2016; first published online 6 November 2016)

Corresponding author G. D. Clarke: Department of Radiology, University of Texas Health Science Center at San Antonio, 7703 Floyd Curl Drive, MC 7800, San Antonio, TX 78229-3900, USA. Email: clarkeg@uthscsa.edu

Abbreviations ALVER, average left ventricular ejection rate; ALVFR, average left ventricular filling rate; ANOVA, analysis of variance; BSA, body surface area; CI, cardiac index (CO/BSA); CMRI, cardiac magnetic resonance imaging; CO, cardiac output; CTL, control group; ED, end-diastolic; EDV, left-ventricular end-diastolic volume; EF, LV ejection fraction; ES, LV end-systolic; ESV, LV end-systolic volume; IUGR, intrauterine growth restriction; LV, left ventricle; MAP, mean arterial pressure; MM, LV myocardial mass; MRI, magnetic resonance imaging; NS, non-significant; OLD, elderly group; pWT, peak LV wall thickness; PLVER, peak left ventricular ejection rate; PLVFR, peak left ventricular filling rate; SI, sphericity index; %WT, percent LV wall thickening.

Introduction

The developmental programming hypothesis postulates that various maternal challenges during fetal and neonatal development, such as hypoxia (Giussani & Davidge, 2013), suboptimal maternal nutrition (Langley-Evans, 2015), maternal obesity and over-nutrition (Zambrano & Nathanielsz, 2013; Taylor *et al.* 2014), alter offspring phenotype, predisposing to a wide variety of adult-onset conditions including hypertension and cardiovascular disease (Barker *et al.* 1989; Hanson & Gluckman, 2014; Thornburg, 2015). Reduced maternal nutrition is the most extensively studied programming challenge and, in experimental models, generally results in fetal intrauterine growth restriction (IUGR) and programming of hypertension and other cardiovascular disorders (Fowden *et al.* 2006; Yeung *et al.* 2014; Langley-Evans, 2015). However, much less is known about the effects of this important programming challenge directly on the heart. The Harvard nurses study, one of the first human epidemiological studies that addressed programming resulting from low birth weight, showed an increased incidence in stroke and heart disease associated with low birth weight (Rich-Edwards *et al.* 1997). Developmental programming is now a topic of major human health interest in the context of gene–environment interactions and the view that the epigenome is fundamental to life course expression of phenotype (Fowden *et al.* 2006; Sun *et al.* 2013; Tarrade *et al.* 2015).

Cardiac dysfunction can be detected *in utero* and in neonatal life in human IUGR offspring (Fouzas *et al.* 2014). However, understanding of IUGR-induced cardiac programming remains limited. Some measures of compromised cardiovascular function are inversely correlated with birth weight (Ward *et al.* 2004; Jones *et al.* 2008). Adult humans exposed to IUGR at term had higher systolic blood pressure and smaller aortic dimension by ultrasound, changes with potential negative consequences for future left ventricular performance (Bjarnegård *et al.* 2013). A better understanding of the underlying pathogenesis will allow development of imaging biomarkers for diagnosis and offer more timely treatment options.

Human epidemiological studies are inherently limited by lifestyle and environmental confounds that vary between individuals. Specifically, in the study of heart disease variations in diet, other lifestyle choices, and various comorbid conditions, such as obesity and diabetes, can limit our understanding of the individual variables responsible for specific long-term outcomes. Many insights on programming of cardiovascular function by IUGR have been carried out in polytocous altricial rodents and polytocous pigs and sheep (Langley-Evans, 2013). However, both reproductive and cardiovascular physiologies in these species are very different from humans.

Non-human primate experimental models are indispensable for advancing fundamental knowledge in biomedical research due to their similarities in cardiovascular physiology, reproduction, and development to humans (Mastorci *et al.* 2009; Shively & Clarkson, 2009). Recently we have developed the baboon as a model for IUGR studies (Nathanielsz *et al.* 2009, Cox *et al.* 2013) developing offspring cohorts of baboon mothers fed *ad libitum* (control, CTL) or 70% *ad libitum* feed in pregnancy and lactation (IUGR). Both male and female offspring of restricted mothers were IUGR, weighing 89% of control offspring at birth (Li *et al.* 2013*b*) and showed programming of their phenotype, e.g. altered cognitive (Keenan *et al.* 2013) and metabolic function (Choi *et al.* 2011).

In addition to its direct effects on the heart, several investigators have hypothesized that programming accelerates ageing (Rodríguez-González *et al.* 2014; Tarry-Adkins and Ozanne, 2014; Alexander *et al.* 2015; Zambrano *et al.* 2015). In this study we investigated the hypothesis that IUGR in our baboon model produces measurable maladaptive cardiac physiology changes with similarities to normal cardiac ageing. Our aim was to demonstrate that moderate nutrient reduction during perinatal development alters cardiac structure and function, leading to abnormal cardiac remodelling. We used cardiac magnetic resonance imaging (CMRI), a well-established method of delineating cardiac changes of ageing and subclinical heart disease in humans (Hees *et al.* 2002; Thiele *et al.* 2002; Maceira *et al.* 2006*a,b*; Germans *et al.* 2007). Our aim was to assess subclinical biomarkers

for impaired cardiac function in young adult IUGR, age-matched controls and elderly baboons in an attempt to uncover similarities and differences in programming by IUGR to the mechanisms of normal ageing.

Methods

Ethical approval

All procedures were approved by the University of Texas Health Science Center and Texas Biomedical Research Institute Institutional Animal Care and Use Committees (IACUC) and conducted in Association for Assessment and Accreditation of Laboratory Animal Care approved facilities. The IACUC is accredited by the Association for Assessment and Accreditation of Laboratory Animal Care International.

Animal model

Baboons (*Papio* species) were studied. Baboons were maintained in an outdoor group social environment and fed using an individual feeding system described previously in detail (Schlabritz-Loutsevitch *et al.* 2004). Healthy gravid female baboons of similar age and weight were randomly assigned to an *ad libitum* diet during pregnancy and lactation or a globally reduced diet regimen consisting of 70% of feed eaten at the same stage of gestation by control *ad libitum* fed mothers from 0.16 gestation (G) (Li *et al.* 2013a).

Blood pressure measurement and calculation

Blood pressure data were acquired in the IUGR and CTL groups with the Omron HBP-1300 professional blood pressure monitor, using either a small (17–22 cm) or a medium (22–32 cm) cuff as appropriate. Prior to blood pressure measurement, baboons were isolated and sedated with intramuscular ketamine injection (10 mg kg⁻¹). Each baboon was placed in the supine position and the cuff positioned on the upper left arm. Blood pressure measurements began within 6 min of ketamine injection. Six measurements were made on each subject, separated by 1–2 min, with the cuff completely loosened. Measurements could not be made on one IUGR female, due to ketamine insensitivity. Mean arterial pressure (MAP) was calculated as the average blood pressure divided by the number of cardiac cycles.

Cardiac magnetic resonance imaging

Cardiac magnetic resonance imaging (CMRI) was performed on three groups of baboons, young adult IUGR baboons (IUGR, $n = 16$, 8 male and 8 female, aged 5.7 ± 1.3 years), age matched control baboons (CTL, $n = 16$, 8 male and 8 female, aged 5.6 ± 1.3 years), and

elderly adults baboons (OLD, $n = 12$, 6 male and 6 female, aged 15.9 ± 3.1 years). Although a direct comparison is not possible across the whole life span, it is usual to multiply baboon age by a factor of 3.5–4 to obtain an approximate human age. To account for potential significant diurnal effects on cardiovascular function, the studies were always conducted at the same time of the day, in the morning (09.00–12.00 h). Subject baseline data are shown in Table 1.

CMRI was performed under isoflurane general anaesthesia. Anaesthesia was induced by ketamine hydrochloride (12 mg kg⁻¹, I.M.) followed by maintenance with isoflurane (0.8–1.0 vol%). Oral intubation was performed following anaesthesia induction for mechanical ventilation. Subsequently, cannulation of the right saphenous vein for i.v. access was performed. Body temperature was maintained with a custom-built feedback-regulated circulating water blanket. Continuous physiological parameter monitoring included measurements of rectal temperature, P_{O_2} , end-tidal P_{CO_2} , electrocardiogram (EKG), blood pressure, heart rate and respiratory rate were continued throughout as well as visual assessment for respiration, voluntary movement and mucosal coloration. Mechanical ventilation was performed at approximately 10 strokes min⁻¹ and 120–180 ml stroke⁻¹. In limited sequence acquisitions where breath-hold was required, a brief interval of hyperventilation was performed following by a brief period of ventilation suspension, not exceeding 30 s in duration. Prompt resumption of ventilation support was achieved following breath-holds. Mechanical ventilation and physiological monitoring were performed using MRI-compatible machines.

All studies were performed on a 3.0 T MRI scanner (TIM Trio, Siemens Healthcare, Malvern, PA, USA) with a six-channel anterior phased-array torso coil and corresponding posterior coil elements, resulting in an aggregate of up to 12 channels of data. Before each imaging session, a standard quality control phantom was scanned. Functional CMRI was performed using steady-state free precession CMRI sequences. High temporal resolution cine CMRI with retrospective gating was performed (repetition time/echo time 3.0/1.5 ms, 25 cardiac phases, matrix 144×192 , field of view 188×250 mm²). Two 3-slice, cine long-axis data sets, in a right anterior oblique view and a four-chamber view, were acquired. Afterwards, a stack of 20–24 contiguous short-axis slices (2.5 mm thickness, no gap) was acquired serially during repetitive breath-holds at end expiration.

On conclusion of the CMRI scanning, isoflurane administration was discontinued, and the subject was slowly weaned to room air and transported to the recovery area. Measurements of heart rate, EKG, temperature, blood pressure, P_{O_2} and end-tidal CO_2 were continued during the entire study. Upon extubation, visual assessment of the animal for respiration, mucosal

Table 1. Baseline characteristics of subjects for CMRI study (mean \pm SD)

Characteristic	CTL		OLD		IUGR		ANOVA
	M	F	M	F	M	F	
Number	8	8	6	6	8	8	—
Age (years)	5.4 \pm 1.4	5.7 \pm 1.3	18.2 \pm 2.6	13.6 \pm 1.4	5.9 \pm 1.2	5.5 \pm 1.4	—
Weight (kg)	19.5 \pm 6.8	13.9 \pm 2.1	31.4 \pm 7.5	17.2 \pm 2.2	21.6 \pm 4.3	13.4 \pm 1.2	G*** S***
Body surface area (m ²)	0.55 \pm 0.13	0.44 \pm 0.04	0.77 \pm 0.12	0.51 \pm 0.04	0.60 \pm 0.08	0.44 \pm 0.03	G*** S****
Birth weight (kg)	0.93 \pm 0.14	0.89 \pm 0.10	NA	NA	0.82 \pm 0.08	0.74 \pm 0.14	G**

G, group difference; S, sex difference; * $P < 0.05$; ** $P < 0.01$; *** $P < 0.001$; **** $P < 0.0005$; NA, not available. See Discussion for age disparity of the OLD group.

coloration and movement was performed at regular intervals not exceeding 15 min in duration until the animal was alert, in a sternal position and demonstrated control of voluntary movement. After the experiments, the subjects were returned to the group baboon facilities. Given CMRI is a non-invasive procedure, there was only minimal blood loss from I.V. access. Of note, the IUGR and CTL baboons have been maintained alive and will be investigated in future CMRI studies while the OLD animals have been transferred to independent studies.

Cardiac image analyses

The CMR⁴² image analysis package (Circle Cardiovascular, Calgary, Alberta, Canada) was used for CMRI data analysis. The left ventricular endocardial and epicardial contours were traced using a semiautomatic algorithm in a time-resolved manner, which resulted in a working left ventricle model (Fig. 1). End-diastolic volume (EDV) and end-systolic volume (ESV) were determined by maximum and minimum cavum volumes, with papillary muscles included in the LV cavity volume by convention. Myocardial mass was estimated with empirical myocardial density (1.05 g ml⁻¹) and average of the LV myocardial volumes at end-systole and end-diastole. Ejection fraction (EF) was computed using EDV and ESV. Ejection and filling functions were assessed from the respective maximal and average downslope and upslope of the volume time curves, giving peak LV ejection and filling rates (PLVER, PLVFR) as well as average LV ejection and filling rates (ALVER, ALVFR). Segmentation was performed in accordance with the American Heart Association standard (Cerqueira *et al.* 2002). Peak LV wall thickness (pWT) at end-systole was calculated using a three-dimensional algorithm developed to measure wall thickness always perpendicular to the myocardium, which has been shown to estimate true wall thickness effectively (Buller *et al.* 1997). Wall thickening fraction expressed as a percentage (%WT) was defined as the ratio of the difference between the wall thickness at end-systole and the end-diastolic wall

thickness to the end-diastolic wall thickness (Peshock *et al.* 1989).

The three-dimensional sphericity index (SI) is a measure of myocardial deformation that is used as an index of LV remodelling (Mannaerts *et al.* 2004). For this study, SI was defined as the ratio of the LV volume to the volume of a sphere having the diameter of the LV long axis, as measured from the mitral valve plane to the endocardial margin at the apex. The larger the SI, the more spherical the LV.

Parameters based on dimensional measurements were evaluated with reference to the body surface area (BSA) (Glassman *et al.* 1984, Maceira *et al.* 2006a). BSA was estimated using weight based models developed from baboon studies as previously described (Leigh, 2009). For female baboons:

$$BSA[m^2] = 0.078(\text{weight}[kg])^{0.664}$$

and for males,

$$BSA[m^2] = 0.083(\text{weight}[kg])^{0.639}.$$

Statistics

Data were analysed using R 3.2.1 statistical software (R Core Team, 2013) and GraphPad Prism 6 (GraphPad Software, Inc., La Jolla, CA, USA) and presented as means \pm standard deviation (SD) unless stated otherwise. In boxplot figures, error bars denote the minimum and maximum, and the boxes indicate the 25th to 75th percentiles with median values represented by a heavy line in the box. Furthermore, the mean is denoted by a plus sign, and potential outliers by Tukey's rule are depicted as individual data points. In cases where suspected outliers are present by Tukey's rule graphically, we performed Grubbs's test (extreme Studentized deviate) to determine if a true outlying point exists. The displayed n values in the figures indicate the number of subjects included in the analysis after exclusion of outliers. Normality of distribution was assessed by the d'Agostino–Pearson test. Two-way ANOVA was used to evaluate the null hypotheses

that there were no differences between the factors group and sex and no significant interactions. Grouped data are presented as box-and-whisker plots, in which the boxes depict the interquartile range of the data. The whiskers extend over 1.5 times the interquartile range, and black circles depict values that lie outside that range. *Post hoc* multiple comparison corrections were performed using Tukey's honest significance test, giving adjusted (*post hoc*) *P* values. Pearson correlation was performed to evaluate the null hypothesis of no significant associations between parameters within groups, as indicated. Regression lines are shown with dotted 95% confidence bands. Statistical significance was set at $P < 0.05$.

Results

Animal model

General characteristics of the CTL, OLD and IUGR groups are shown in Table 1. The IUGR baboons demonstrated decreased birth weight compared to age-matched controls ($P < 0.01$). The difference in body weight between the CTL and IUGR groups was no longer apparent by young adulthood. Birth weights for the OLD group were unavailable.

Contraction-relaxation timing and blood pressure measurements

Timing parameters for the CMRI study are shown in Table 2. A significantly higher resting heart rate was measured in females, which was present in all groups. The duration of diastole was increased in the IUGR group relative to CTL ($P < 0.05$), but no sex effect was evident. Although diastolic duration was also longer in OLD, significance was not reached in OLD relative to CTL. No difference was seen between groups in systolic duration. There were no differences in systolic blood pressure, diastolic blood pressure, or MAP between the IUGR and CTL baboons (Table 3). Resting heart rate in female baboons was again significantly greater than in males during the blood pressure measurements ($P < 0.01$).

Left ventricular function and morphology

CMRI-measured LV functional parameters are presented in Table 4 for the CTL, OLD and IUGR groups. Left ventricular parameters that differed only between groups included EF, end-systolic (ES)-SI, end-diastolic (ED)-SI, cardiac index (CI; cardiac output (CO)/BSA), ESV/BSA, pWT/BSA, and ALVFR/BSA. In the OLD and IUGR

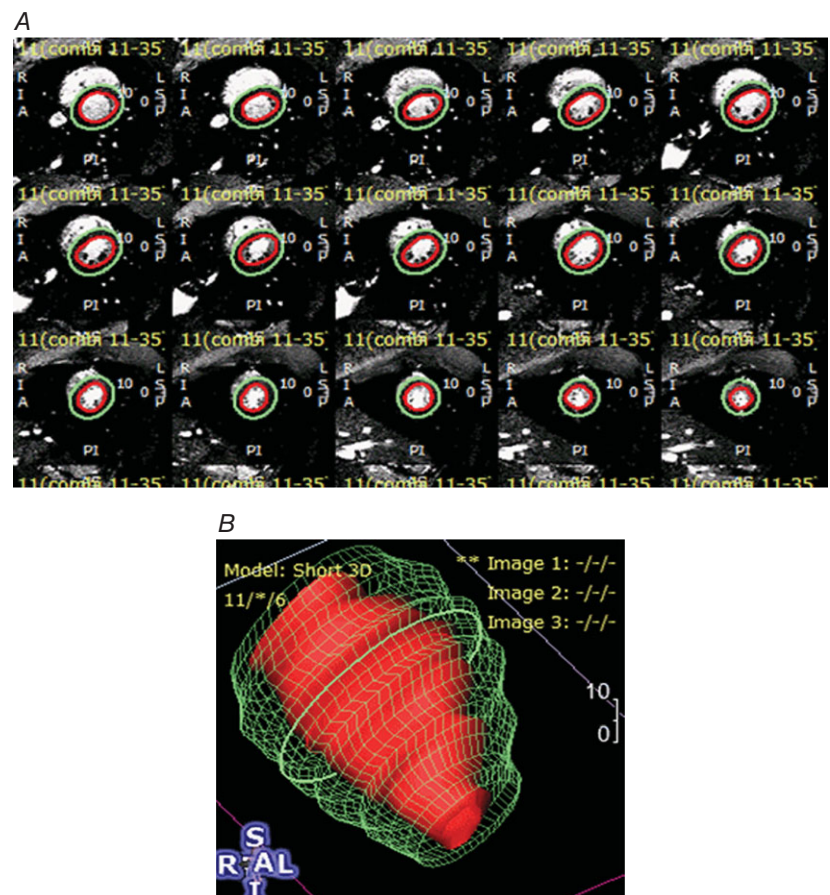


Figure 1. A. Short axis sections of cardiac temporal phases (columns) and slices (rows). B. Wire frame display shows volumetric reconstruction of LV

A, cardiac motion was measured by imaging 25 phases of the cardiac cycle. Subepicardial and subendocardial margins were drawn using a semiautomated algorithm with manual adjustment and visual confirmation. B, wireframe reconstructions were produced and depicted. Results of ventricular volume and wall motion analyses are presented in Table 4.

Table 2. Cardiac MRI timing parameters (mean \pm SD)

Parameter	CTL		OLD		IUGR		ANOVA	Post hoc
	M	F	M	F	M	F		
Heart rate (bpm)	95 \pm 7	108 \pm 17	89 \pm 8	97 \pm 13	91 \pm 16	94 \pm 15	S*	
Time in systole (ms)	252 \pm 34	257 \pm 62	277 \pm 50	245 \pm 30	269 \pm 59	246 \pm 40	NS	
Time in diastole (ms)	385 \pm 28	309 \pm 44	402 \pm 36	385 \pm 85	412 \pm 86	406 \pm 89	G*	CTL < IUGR*
Diastole to systole ratio	1.5 \pm 0.2	1.3 \pm 0.3	1.5 \pm 0.3	1.6 \pm 0.4	1.6 \pm 0.3	1.7 \pm 0.3	NS	

NS, non-significant; G, group difference; S, sex difference; * $P < 0.05$. No significant sex-group interaction was seen.

Table 3. Non-imaging parameters (mean \pm SD)

GROUP	CTL		IUGR		ANOVA
	M (n = 8)	F (n = 8)	M (n = 8)	F (n = 7)	
Heart rate (bpm)	111 \pm 12	135 \pm 13	112 \pm 13	130 \pm 11	S**
Systolic BP (mmHg)	118 \pm 16	116 \pm 27	113 \pm 19	119 \pm 13	NS
Diastolic BP (mmHg)	68 \pm 22	71 \pm 26	63 \pm 23	66 \pm 10	NS
MAP (mmHg)	85 \pm 20	86 \pm 26	80 \pm 22	84 \pm 11	NS
Body temperature ($^{\circ}$ F)	39.17 \pm 0.61	38.56 \pm 0.61	38.94 \pm 0.44	38.94 \pm 0.44	NS

BP, blood pressure; MAP, mean arterial blood pressure; NS, non-significant; S, sex difference; ** $P < 0.01$. No significant between group difference or sex-group interaction was seen.

groups, EF was lower than CTL (P_{OLD} : NS, $P_{\text{IUGR}} < 0.01$) and both ES-SI (P_{OLD} : NS, $P_{\text{IUGR}} < 0.001$) and ED-SI ($P_{\text{OLD}} = 0.001$, $P_{\text{IUGR}} < 0.01$) were higher compared to CTL, with the ES-SI values of the IUGR being markedly larger than either CTL or OLD groups (Fig. 2). The apparent outlier by Tukey's rule in the CTL group was determined to be not a statistically significant outlier by Grubbs's test. Statistical outliers were identified in the IUGR group with ejection fraction and end-diastolic sphericity index (Fig. 2). After removal of these outliers, normality of distribution was found in all measured parameters. The statistical values, described above, were obtained after removal of the outlier. However, for the sake of completeness, those values are left in place in the graphical figures.

A difference between groups in cardiac index (CO/BSA) was present by ANOVA due to the combined effect of decreased CI in the IUGR ($P = 0.02$) and OLD ($P = 0.04$) groups compared to CTL (Fig. 3A). Grubbs's test confirmed the presence of an outlier in the IUGR group, which was excluded from analysis. On the other hand, the apparent outlier in the CTL group was determined by Grubbs's test to not be a statistically significant outlier. Normalized ESV/BSA was higher in the IUGR group ($P < 0.05$, Fig. 4A). Normalized pWT was also lower in both the IUGR ($P < 0.05$) and OLD groups ($P < 0.01$) compared to CTL (Fig. 3B). ALVFR/BSA was lower in IUGR ($P < 0.05$) and OLD ($P < 0.05$) relative to CTL. Lower PLVFR values, seen in the IUGR and

OLD group compared to CTL, approached significance ($P = 0.09$).

The parameters with between-sex differences were further sub-analysed and are displayed in Table 5. Left ventricular parameters that differed by sex only after normalization to BSA included stroke volume and end-diastolic volume. The stroke volumes in females remained smaller than in males in all three groups. Likewise, EDV/BSA was higher in males in all groups. After adjusting to myocardial mass, no significant sex difference persisted.

LV parameters that showed differences by both group and sex factors included myocardial mass (MM)/BSA and %WT. MM/BSA was lower in females compared to males in all three groups ($P_{\text{OLD}} < 0.05$, $P_{\text{CTL}} < 0.05$, $P_{\text{IUGR}} < 0.001$) (Fig. 5). MM/BSA values were lower in the OLD compared to CTL ($P < 0.05$). A similar trend that did not reach significance was noted in IUGR compared to CTL, likely to be due to pronounced variability in the male IUGR group (Fig. 5A). Two-way ANOVA of the %WT values revealed significant differences between groups ($P < 0.005$) and between sexes ($P < 0.01$), but no group-sex interaction. The females demonstrated significantly lower %WT ($P < 0.05$), while the IUGR %WT values were significantly lower than both CTL ($P < 0.001$) and OLD ($P = 0.01$). A significant difference was found both between the CTL males and IUGR males ($P < 0.01$) and between CTL females and IUGR females ($P < 0.05$, Fig. 5B).

Table 4. LV volumes, systolic function, diastolic function and mass parameters (absolute and normalized to BSA, mean \pm SD)

GROUP	CTL (n = 16)	IUGR (n = 16)	OLD (n = 12)	ANOVA	Post hoc
Absolute values					
MM (g)	37.7 \pm 11.1	37.8 \pm 15.7	42.6 \pm 17.5	S***	
SV (ml)	15.4 \pm 6.0	13.0 \pm 5.2	16.0 \pm 9.4	S***	
CO (l min ⁻¹)	1.57 \pm 0.68	1.23 \pm 0.52	1.45 \pm 0.78	S***	
EF (%)	57.6 \pm 12.0	45.2 \pm 8.1	49.8 \pm 12.2	G**	CTL > IUGR**
ESV (ml)	11.4 \pm 5.3	16.2 \pm 8.7	15.4 \pm 8.2	S**	
EDV (ml)	26.8 \pm 10.0	29.3 \pm 13.1	31.5 \pm 15.8	S***	
pWT (mm)	16.2 \pm 3.2	14.3 \pm 3.2	16.1 \pm 2.8	S***	
%WT (%)	47.9 \pm 13.9	30.4 \pm 8.8	43.1 \pm 12.0	G*** S*	CTL > IUGR*** OLD > IUGR***
ESSI (%)	26.4 \pm 6.6	38.9 \pm 8.2	29.6 \pm 7.4	G***	IUGR > CTL*** IUGR > OLD**
EDSI (%)	31.6 \pm 4.4	37.3 \pm 3.3	40.8 \pm 7.0	G***	IUGR > CTL** OLD > CTL***
PLVER (ml s ⁻¹)	110 \pm 55	106 \pm 37	108 \pm 66	S***	
PLVFR (ml s ⁻¹)	99 \pm 38	79 \pm 36	102 \pm 57	S**	
ALVER (ml s ⁻¹)	65 \pm 32	52 \pm 22	61 \pm 34	S**	
ALVFR (ml s ⁻¹)	45 \pm 18	33 \pm 15	41 \pm 22	S**	
Normalized to BSA					
MM/BSA (g m ⁻²)	74.8 \pm 10.7	70.7 \pm 15.8	65.0 \pm 13.6	G* S***	CTL > OLD**
SV/BSA (ml m ⁻²)	30.2 \pm 7.7	24.6 \pm 7.5	24.0 \pm 9.7	G ⁻ S***	
CO/BSA (l min ⁻¹ m ⁻²)	3.1 \pm 1.1	2.2 \pm 0.6	2.2 \pm 0.9	G*	CTL > IUGR* CTL > OLD*
ESV/BSA (ml m ⁻²)	22.3 \pm 7.9	30.4 \pm 11.4	23.2 \pm 8.1	G*	IUGR > CTL*
EDV/BSA (ml m ⁻²)	52.6 \pm 10.4	55.1 \pm 17.1	47.4 \pm 13.7	S*	
pWT/BSA (mm m ⁻²)	33.2 \pm 7.2	27.9 \pm 4.0	25.0 \pm 3.3	G***	CTL > IUGR* CTL > OLD**
PLVER/BSA (ml s ⁻¹ m ⁻²)	219 \pm 103	204 \pm 63	162 \pm 67	NS	
PLVFR/BSA (ml s ⁻¹ m ⁻²)	199 \pm 70	150 \pm 61	154 \pm 61	G ⁻	
ALVER/BSA (ml s ⁻¹ m ⁻²)	127 \pm 54	98 \pm 34	94 \pm 42	NS	
ALVFR/BSA (ml s ⁻¹ m ⁻²)	89 \pm 28	64 \pm 28	62 \pm 25	G*	CTL > IUGR** CTL > CTL*
Normalized to MM					
EDV/MM (ml g ⁻¹)	74.8 \pm 10.7	70.7 \pm 15.8	65.0 \pm 13.6	NS	
SV/MM (ml g ⁻¹)	30.2 \pm 7.7	24.6 \pm 7.5	24.0 \pm 9.7	NS	

NS, non-significant; G, group difference; S, sex difference; -, $P < 0.1$; * $P < 0.05$; ** $P < 0.01$; *** $P < 0.005$. No significant sex-group interaction was found. ALVER, average LV ejection rate; ALVFR, average LV filling rate; CO, cardiac output; EDSi, end-diastolic sphericity index; EDV, end-diastolic volume; EF, ejection fraction; ESSI, end-systolic sphericity index; ESV, end-systolic volume; MM, myocardial mass; pWT, peak wall thickness; SV, stroke volume; PLVER, peak LV ejection rate; PLVFR, peak LV filling rate; %WT, "percent" wall thickening.

Correlation analyses

There was a significant negative correlation of ESV/BSA with percentage wall thickening ($r = -0.4$, $P < 0.01$) across all groups with the scatter plot stratifying the IUGR group as having generally high ESV/BSA and low %WT (Fig. 4B).

Correlation analyses were performed on each group between normalized LV peak filling rates and diastolic sphericity. As shown in Fig. 6A, there was no correlation between these two parameters in CTL ($r = 0.14$, NS). A strong correlation between these parameters ($r = 0.81$, $P < 0.001$) was present in IUGR baboons (Fig. 6B),

which persisted after removing the outlier ($r = 0.87$, $P < 0.0001$). In the OLD group, there was a weaker but significant positive correlation ($r = 0.69$, $P < 0.01$) between PLVFR/BSA and ED-SI (Fig. 6C).

To determine whether cardiac dysfunction, seen in young adulthood, can be traced to the extent of intrauterine growth, interaction plots between birth weights and normalized PLVFR were generated (Fig. 7). A positive correlation was seen between birth weight and

normalized PLVFR in the IUGR group ($r = 0.56$, $P < 0.05$, Fig. 7). No significant correlation was observed in the CTL group ($r = 0.15$, NS).

Discussion

Decreased maternal nutrition in pregnancy and the associated fetal under-nutrition are common challenges to fetal growth and development worldwide and food

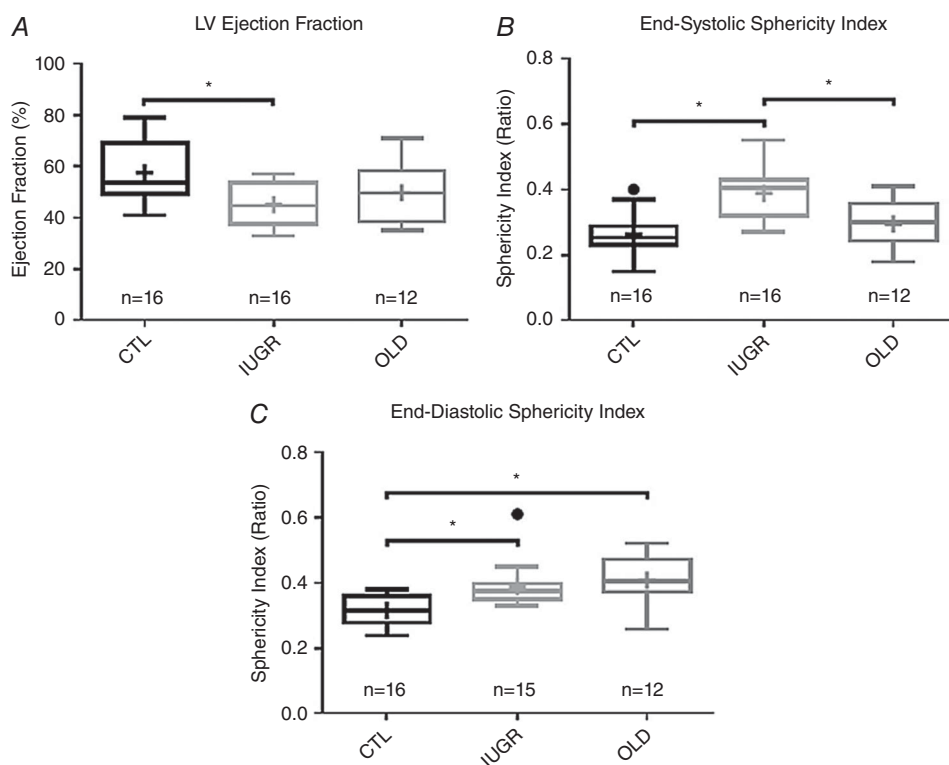


Figure 2. Ejection fraction and LV remodeling in IUGR baboons is similar to older animals

A, significant differences were observed in ejection fraction (EF), with CTL group values being higher than IUGR ($P < 0.01$) and OLD groups (NS). B, compared to CTL, end-systolic sphericity indices were higher in the IUGR group ($P < 0.0001$). C, higher end-diastolic sphericity indices, indicative of ventricular remodelling, were noted in the IUGR ($P < 0.01$) and OLD groups ($P < 0.001$).

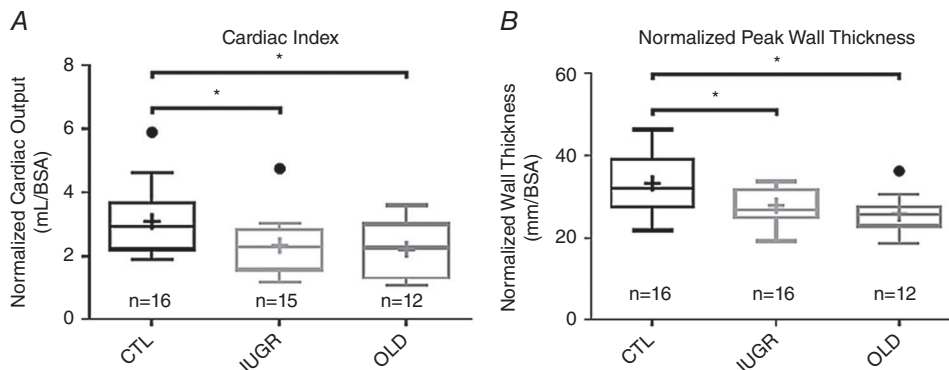


Figure 3. Systolic function is impaired in the left ventricles of IUGR baboons

A, decreased cardiac indices were seen in the IUGR ($P < 0.05$) and OLD ($P < 0.05$) groups compared to CTL. B, normalized LV wall thickness is significantly lower in IUGR ($P < 0.05$) and OLD groups ($P < 0.01$) compared to CTL.

security is a significant problem, even in economically advanced countries (Coleman-Jensen *et al.* 2014; Lambie-Mumford and Dowler, 2014; Pfeiffer *et al.* 2015). IUGR is a very important obstetric complication with an incidence that varies according to socio-economic, ethnic and other factors. The baboon has many strengths as an experimental species to study developmental programming. In terms of maternal physiology, like women, pregnant baboons carry only a single fetus in contrast to polytocous species. This distinction is important in relation to the higher nutritional burden experienced in pregnancy by polytocous compared with monotocous species. In addition, the genetic similarity between baboons and humans, evident in overall DNA sequence and individual gene sequence identity and arrangement of genetic loci on chromosomes, reflects the close evolutionary relationship between these two species (Rogers, 2000).

Our data revealed systolic dysfunction, diastolic dysfunction and remodelling of the left ventricle in baboons that were IUGR as a result of exposure to moderate perinatal maternal nutrient restriction. The systolic dysfunction is characterized by decreased EF, decreased wall thickening, decreased peak wall thickness and decreased cardiac index. Diastolic impairment is marked by reduced LV filling rates, prolonged diastolic filling times, and borderline impaired ventricular relaxation during active filling. LV remodelling is evidenced by increased globular morphology and increased end-systolic and end-diastolic LV volumes. Overall, many of the changes resulting from IUGR parallel those observed in the OLD animals (Table 6). The observed functional differences in the IUGR group are more modest than those characterizing clinical heart failure (Kitzman, 2002) and may better represent the lower limit of the normal functional range, presenting opportunities for early diagnosis of future disease.

However, they are consistent and indicative of a decrease in cardiac function in young adulthood to a level comparable to or even exceeding the effects of later ageing. Even though we examined both male and female baboons, the majority of our findings are not sexually dimorphic after normalization to BSA except for resting heart rate, normalized myocardial mass and fractional wall thickening, which were significantly different by sex.

The results of the current study are consistent with persistent impairment of systolic function and reduced ejection force that have previously been reported in growth-restricted children and fetuses (Rizzo *et al.* 1995; Crispi *et al.* 2010). Likewise, our findings of diastolic dysfunction suggest the previously reported diastolic disturbance and impaired ventricular filling in IUGR human neonates and small for gestational age human fetuses persist into adulthood (Miyague *et al.* 1997; Fouzas *et al.* 2014). While the mechanism underlying those dysfunctions is not yet clearly understood, previous examination on human IUGR fetal myocardial ultrastructure indicates that shortened sarcomere length may contribute to the aberrant ejection function (Iruetagoiena *et al.* 2014). Similarly, in studies of sheep where cardiomyocyte maturation occurs prenatally, as in humans, IUGR and birth weight have been shown to affect the number of cardiomyocytes. The timing of cardiomyocyte maturation is thought to contribute to systolic dysfunction, depending on the method of IUGR induction (Bubb *et al.* 2007; Stacy *et al.* 2009; Botting *et al.* 2014). Additionally, irregular calcium handling and cardiac contraction function have been demonstrated in male nutrient-restricted IUGR rats (Harvey *et al.* 2015). We have reported increased extracellular fibrosis in fetal male IUGR baboon myocardial tissue, which may be related to impaired LV diastolic function (Maloyan *et al.* 2014). While the chronology of dysfunction is difficult to

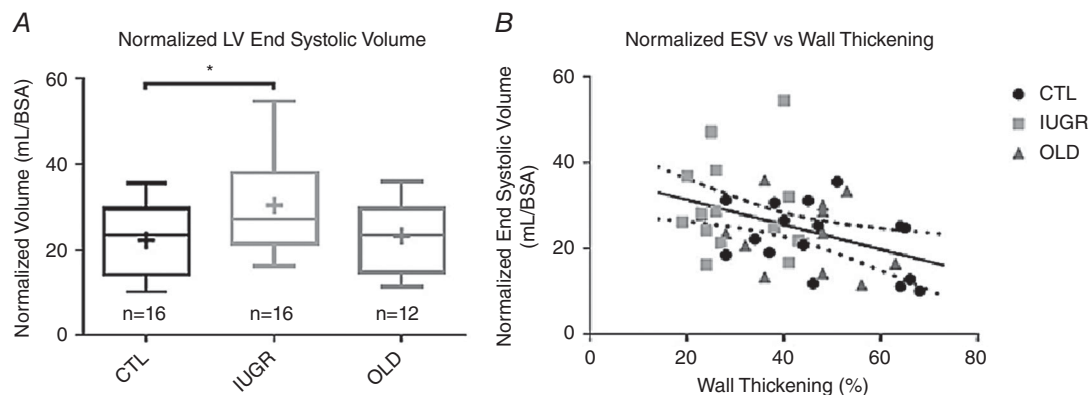


Figure 4. End-systolic LV volume is greater in IUGR baboons and is inversely correlated with percent wall thickening

A, normalized ESV was significantly higher in the IUGR group ($P < 0.05$) compared to CTL. B, there was a significant inverse correlation of ESV/BSA with percentage wall thickening ($r = -0.4$, $P < 0.01$), which exhibited stratification by group. No between group difference in regression slope was found.

Table 5. LV sub-group data by sex

GROUP	CTL (n = 16, 8 M)	IUGR (n = 16, 8 M)	OLD (n = 12, 6 M)
MM (g)			
Male	46.0 ± 10.1	49.6 ± 14.2	56.7 ± 13.9
Female	29.3 ± 2.1	26.0 ± 2.7	28.5 ± 1.9
SV (ml)			
Male	18.6 ± 5.7	16.7 ± 3.2	21.9 ± 9.9
Female	12.2 ± 4.5	9.3 ± 4.0	10.1 ± 3.5
CO (l min ⁻¹)			
Male	1.78 ± 0.67	1.57 ± 0.24	1.90 ± 0.81
Female	1.36 ± 0.66	0.90 ± 0.53	1.01 ± 0.45
ESV (ml)			
Male	11.8 ± 6.4	20.1 ± 9.8	20.5 ± 8.7
Female	11.1 ± 4.5	11.7 ± 4.0	10.3 ± 3.2
EDV (ml)			
Male	30.5 ± 11.2	37.7 ± 12.4	42.6 ± 15.6
Female	23.2 ± 7.5	20.9 ± 7.5	20.4 ± 4.0
pWT (mm)			
Male	18.6 ± 2.4	15.9 ± 3.5	17.8 ± 2.5
Female	13.8 ± 1.5	12.7 ± 1.7	14.4 ± 2.2
%WT (%)			
Male	54.8 ± 12.1	34.4 ± 9.2	47.3 ± 10.3
Female	40.9 ± 12.2	26.4 ± 7.1	39.2 ± 13.2
PLVER (ml s ⁻¹)			
Male	132 ± 49	128 ± 27	142 ± 80
Female	87 ± 54	83 ± 33	74 ± 22
PLVFR (ml s ⁻¹)			
Male	109 ± 26	100 ± 20	135 ± 63
Female	89 ± 47	59 ± 37	69 ± 25
ALVER (ml s ⁻¹)			
Male	77 ± 32	65 ± 18	79 ± 36
Female	52 ± 30	39 ± 18	43 ± 20
ALVFR (ml s ⁻¹)			
Male	49 ± 17	42 ± 9	53 ± 23
Female	41 ± 18	25 ± 17	28 ± 13
MM/BSA (g m ⁻²)			
Male	83.3 ± 6.6	81.7 ± 15.1	73.9 ± 14.2
Female	66.3 ± 5.9	59.7 ± 5.5	56.0 ± 3.5
SV/BSA (ml m ⁻²)			
Male	33.2 ± 4.4	28.0 ± 4.0	27.9 ± 10.4
Female	27.2 ± 9.2	21.2 ± 8.8	20.2 ± 7.9
EDV/BSA (ml m ⁻²)			
Male	53.8 ± 8.2	62.2 ± 14.9	54.5 ± 14.5
Female	51.4 ± 12.7	48.0 ± 17.0	40.4 ± 9.1

ALVER, average LV ejection rate; ALVFR, average LV filling rate; CO, cardiac output; EDSi, end-diastolic sphericity index; EDV, end-diastolic volume; EF, ejection fraction; ESSI, end-systolic sphericity index; ESV, end-systolic volume; MM, myocardial mass; pWT, peak wall thickness; SV, stroke volume; PLVER, peak LV ejection rate; PLVFR, peak LV filling rate; %WT, "percent" wall thickening.

assess due to the intricate interactions of the cardiovascular system, it is interesting to note that the reduced birth weights produced by our methods correlated best with poorer filling function, hinting that diastolic dysfunction may be a primary effector. This trend toward impaired diastolic function has previously been noted in chick embryos incubated under hypoxia (Itani *et al.* 2016).

This is the first study on effects of any degree of perinatal under-nutrition on adult offspring cardiac function in a non-human primate model. Our model offers many advantages, including well-controlled degree of nutritional challenge, matching of the maternal phenotypes (Li *et al.* 2013b), the presence of a single fetus and offspring to rear in baboons compared to the

large litters in polytocous species (including rodents), genetic similarity to humans (Rogers *et al.* 2000), and precocial fetal and neonatal development that results in a developmental trajectory closer to that of humans. The ability to precisely induce IUGR and control groups experimentally provides further benefits over a similar

study on a large cohort of humans, where many confounders (e.g. smoking and different diets) must be taken into account. Most published animal studies on cardiac function in the setting of perinatal nutrient restriction have focused on rat models of IUGR, with a few studies reported on mice (Kawamura *et al.* 2007;

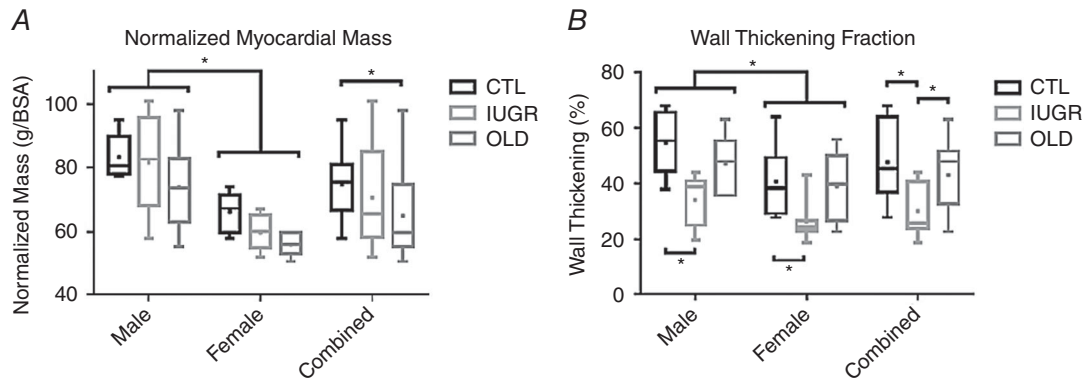


Figure 5. Sex-related differences in normalized myocardial mass and percent wall thickening
 A, normalized myocardial mass was significantly lower in female baboons compared to males ($P < 0.005$). A significant difference between groups was also found by ANOVA ($P < 0.05$). B, percentage wall thickening also revealed sex differences ($P < 0.01$) and group differences ($P < 0.005$) by ANOVA.

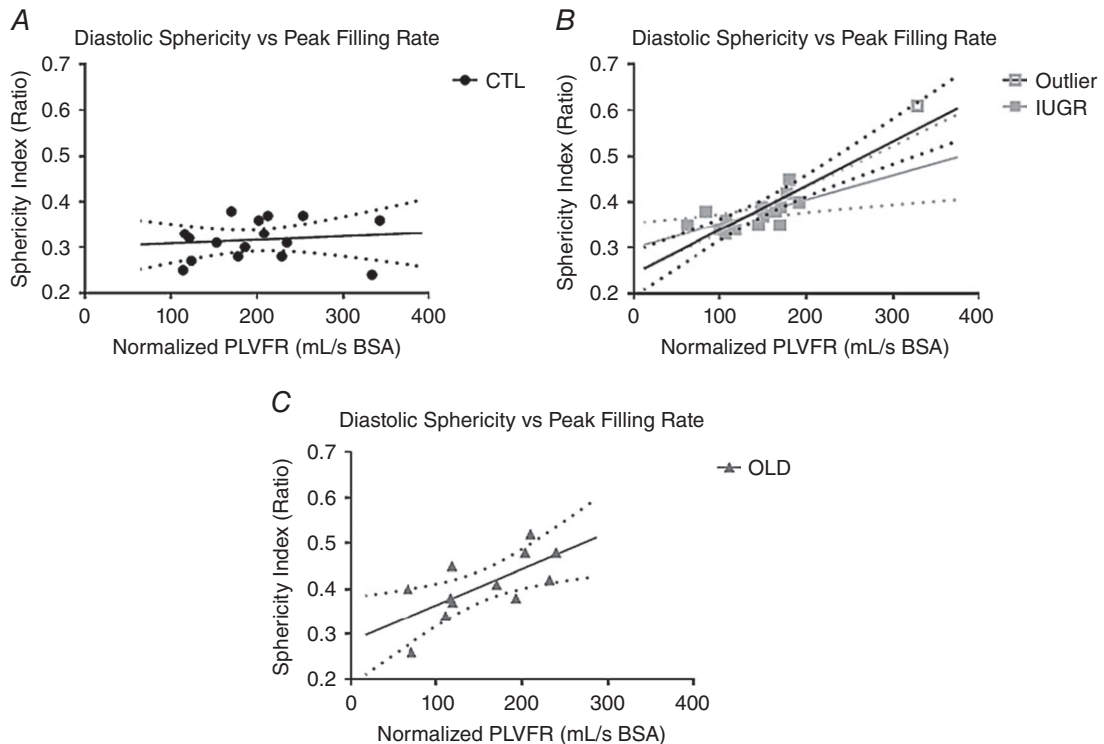


Figure 6. An association between remodeling and diastolic function in IUGR and OLD groups was not evident in controls
 No association was found between the BSA-normalized peak left ventricular filling rates and three-dimensional diastolic sphericity indices in CTL baboons ($r = 0.14$, NS; A) but highly significant associations were found between 3D-DSI and LVFR/BSA in IUGR baboons ($r = 0.81$, $P = 0.001$; B) and OLD baboons ($r = 0.69$, $P < 0.01$; C). An outlier is identified in the IUGR group, exhibiting both higher than normal normalized PLVFR and 3D-DSI. After excluding this outlier, the correlation remains significant ($r = 0.87$, $P < 0.0001$); regression line shown before (black) and after (grey) removal of the outlier.

Cai *et al.* 2012), rabbits (Gonzalez-Tendero *et al.* 2013), chicks (Itani *et al.* 2016) and sheep (Stacy *et al.* 2009; Botting *et al.* 2014). While the results regarding IUGR cardiac function have not always been entirely congruent, we should keep in mind that many aspects of development differ across species and the method for IUGR induction often also differ across studies. Historically, the major interventions that have been used to produce experimental IUGR include hypoxia, procedural interruption of uterine function or vascular supply, malnutrition (often in the form of a low-protein maternal diet), and global under-nutrition to various extents, as in the present study. There is particular interest in comparing the results of the present study with those from the body of work that focused on directly measuring the effects of IUGR on cardiac function in other models. *Ex vivo* Langendorff perfusion heart studies have been conducted to examine influences of IUGR on myocardial function in a setting that aims to address intrinsic factors within the heart and remove extra-cardiac factors.

Using the ischaemia–reperfusion paradigm, impaired IUGR cardiac function recovery is noted in at least two of these studies, cementing the notion of abnormal cardiac health with IUGR (Xu *et al.* 2006; Rueda-Clausen *et al.* 2010). In the study by Xu *et al.* (2006) effects of both hypoxia and nutrient restriction IUGR are compared. The myocardia of animals in both treatment groups developed thickening of the extracellular matrix. Diastolic dysfunction was impaired, and LV end-diastolic pressures increased, in line with our observation of diastolic dysfunction. In another report of hypoxia-induced IUGR in male rats, a significant increase in the LV ejection pressure rate and increased rate–pressure product were noted compared to controls, consistent with decline in cardiac performance and increase myocardial work load (Giussani *et al.* 2012). These observations also agree with our findings. Offspring systolic and diastolic dysfunction

are both noted in the hypoxic IUGR chick model, as well as decreased LV wall to lumen ratio and wall volume, similar to our findings (Itani *et al.* 2016). Rueda-Clausen *et al.* (2010) demonstrated increased normalized heart weight in their hypoxia-induced IUGR male rats, but not female rats, a finding we did not observe with the moderate nutritional challenge in the baboon. However, we note that LV hypertrophy is observed in the hypoxia group but not with nutrient restriction in the study of Xu *et al.* (2006), in agreement with the lack of effect on normalized myocardial mass seen in our study. In the chick model, a difference in heart weight is not seen after normalization to embryo weight (Itani *et al.* 2016). Furthermore, Xu *et al.* reported an apparent delay in remodelling of the nutrient restriction group (visible at 7 months) compared to the hypoxia group (visible at 4 months), further confirming there are key differences in timing and degree of outcomes in response to the various challenges that produce IUGR. This is not surprising and, while it suggests caution in interpreting the different outcomes, the variability also may provide clues to both common and different mechanisms.

Results from *in vivo* cardiac functional studies of IUGR are mixed. In the study by Cheema *et al.* (2005) in a low-protein rat model, a minimally thinner LV wall was noted in the low-protein group along with severely depressed EF up to only 2 weeks of age, after which the ventricular wall progressively thickened, exceeding that of controls, and EF normalized. A more spherical morphology of the heart was reported but only to 12 weeks of age, not up to 28 more weeks after. In the rat study by Mendendez-Castro *et al.* (2014), however, low protein IUGR decreased EF, increased end-systolic and end-diastolic diameters, and decreased wall thickness discernible at 70 days of age. In studies by Zohdi *et al.* (2011, 2013, 2014) with a protein restriction rat model, no baseline cardiac dysfunction was evident in the low protein IUGR group at 14 weeks of age except for reduced end-diastolic volume, but attenuated stroke volume and cardiac output were seen with a dobutamine challenge, and myocardial tissue had increased lipid, proteoglycan and carbohydrate content compared to controls. Together, these studies suggest the development of functional cardiac impairments may occur in stages in the various rodent studies, but preclude direct and meaningful comparisons to our findings. Furthermore, we again note that the physiology of IUGR by protein restriction *versus* moderate nutrient restriction should not necessarily be considered equivalent.

The LV remodelling observed in our model manifests as a more globular morphology. This finding has been previously reported in other IUGR models. The positive correlation between end-diastolic sphericity index and peak filling rate in the IUGR and OLD groups is interpreted as a compensatory morphological acclimation

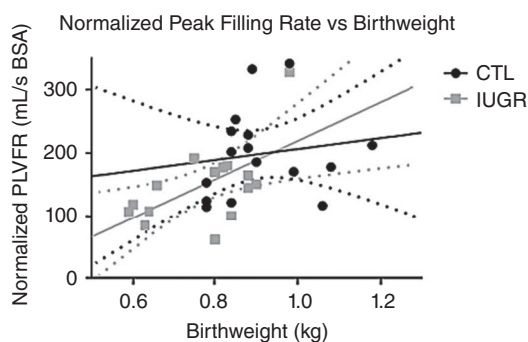


Figure 7. Diastolic function is associated with birth weight in IUGR animals but not in controls

A positive association was noted between the normalized peak LV filling rate and birth weight in the IUGR group (grey, $r = 0.56$, $P = 0.02$). No association was found between the normalized peak LV filling rate and birth weight in the CTL group (black, $r = 0.15$, NS).

Table 6. Cardiovascular parallels and dissimilarities between IUGR and ageing

Measurement	IUGR	OLD
Similarities		
Time in diastole	Increased	Similar trend, not reaching significance
Ejection fraction	Decreased	Similar trend, not reaching significance
LV wall thickening	Decreased	Similar trend, not reaching significance
End-diastolic sphericity index	Increased	Increased
Normalized myocardial mass	Similar trend, not reaching significance	Decreased
Cardiac index	Decreased	Decreased
Normalized peak wall thickness	Decreased	Decreased
Normalized peak filling rate	Similar trend, not reaching significance	Similar trend, not reaching significance
Normalized average filling rate	Decreased	Decreased
Dissimilarities		
End-systolic sphericity index	Increased	No significant change
Normalized end-systolic volume	Increased	No significant change

that leads to preservation of the filling function. A similar globular appearance of the ventricle has been reported in both human IUGR fetuses and rodent models (Crispi *et al.* 2010, 2014; Menendez-Castro *et al.* 2014). Remarkably, whereas increased end-systolic sphericity index and associated elevated normalized end-systolic volume were observed with IUGR, no similar appreciable change was noted in the OLD animals. We speculate that the end-systolic differences between IUGR and OLD may be partially attributed to the physiological algorithm that controls remodelling and compensation. Compared to the gradual process of ageing, the results from other studies indicate that the stress of IUGR physiology starts early and may consist of more radical modifications. It is possible that while the LV of the OLD animals can gradually accommodate for the decreased systolic function via ventricular hypertrophy to increase contractility, rapid IUGR LV development prohibits this type of acclimation. Even though not suggestive of this hypothesis, the relative sparing of the ejection fraction, increased peak wall thickness, and increased wall thickening fraction in OLD animals are supportive of this premise. It will be of interest to re-examine the IUGR baboon hearts at a later time point to see whether such compensatory thickening of the LV wall occurs given sufficient time. Progressive thickening of the thinner IUGR LV wall with age accompanied by normalization of EF has been previously reported in a rodent study (Cheema *et al.* 2005). However, in that experiment, EF normalizes and wall thickness exceeds normal by adulthood.

There are a number of differences in the cardiac function parameters measured in this baboon model compared to those previously reported in adult reduced-protein IUGR rat models. In one study, no differences between IUGR and control groups were found in the values of CO, SV, or LV cardiac dimensions (Zohdi *et al.* 2011). In another study, no differences were reported between male IUGR and

male controls for CO, LV wall size, and internal diameters during systole and diastole, yet MAP was increased and the rate of change in pressure were down during LV ejection and filling (Cheema *et al.* 2005). We suspect the difference in our findings may partly originate from differences in analytic technique. The heart weights of the above-mentioned studies have been reported as decreased in the IUGR groups, whereas we have only observed a trend of decrease myocardial mass after normalization to BSA. We note that BSA-adjusted measurements of heart function are not typically performed in rodent studies of cardiac function. In humans, multivariate analyses have shown that BSA is a significant independent variable influencing many CMRI cardiac parameters (Maceira *et al.* 2006b). Nonetheless, this difference in technique does not account for the lack of EF difference detected by those studies. It is unclear whether physiological differences between rodents and primates, types of IUGR interventions used and differences in precisions of the measurements further complicate the comparison.

Many previous studies on cardiovascular effects of IUGR models have focused on measuring blood pressure, often reporting hypertension in the affected offspring. Various hypotheses have been generated involving epithelial dysfunction, abnormal vascular smooth muscle characteristics and change in myocardial tissue properties, such as reduced vasodilatation capacity leading to hypertension (Brawley *et al.* 2003) and aortic wall thickening leading to impaired vascular reactivity (Camm *et al.* 2010). The losses in cardiac function that we found in this study and attributed to IUGR are present in the absence of hypertension. Due to the prevalence of hypertension in many human epidemiological and rodent IUGR studies, there has long been an assumption that cardiac impairment is secondary to hypertension in IUGR (Alexander *et al.* 2015). However, the evidence for the dependence of heart function on hypertrophy in protein deprived rat models

has been mixed, similar to recent rat models that try to account for the physiological differences between rats and humans (Zohdi *et al.* 2014). Given our results, if hypertension is an immediate consequence in the moderately nutrient-restricted IUGR baboons, it is either below the threshold of detection or moderated over time and absent by adulthood. Further, given that blood pressure varies greatly with stress, anaesthesia and timing, we have to consider that the previous measurements of hypertension in IUGR models were measured under conditions with very different physiological states.

We hypothesize that in our model, the development of impaired myocardial function without chronic hypertension is due to the development of diffuse myocardial fibrosis. Stiffening of the myocardium and impaired systolic and diastolic functions are known consequences of increased fibrotic tissue deposition (Weber *et al.* 1993). In addition, a shortening of myocardial sarcomeres may have occurred, further compromising systolic function (Iruetagoiena *et al.* 2014). We speculate that to ameliorate LV relaxation failure due to decreased compliance, structural expansion of the LV occurs, preserving the EDV and decreasing wall stress while developing a globular ventricular morphology (Fig. 8). The adaptive feature of this remodelling is supported by the positive correlation found between peak diastolic filling rate and diastolic sphericity index (Fig. 7). These intra-cardiac changes are likely to be part of a more comprehensive response

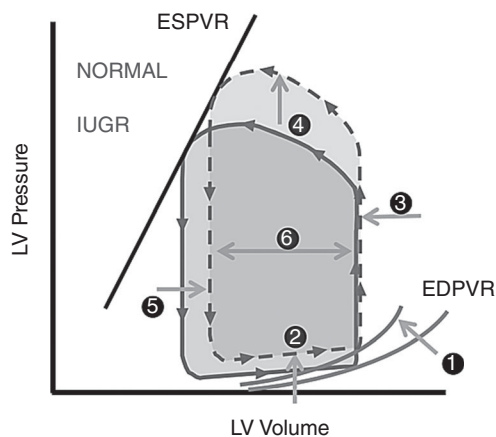


Figure 8. Proposed pressure–volume loop model of IUGR cardiac pathophysiology

Myocardial fibrosis results in altered end-diastolic pressure–volume relationship (EDPVR; 1). Increased pressure is thus required for diastolic filling (2). Increased ventricular cavity size and concomitant decreased ventricular compliance result in minimal end-diastolic volume change (3). Increased afterload is observed in IUGR, as previously documented (4). Combined effects of increased afterload, increased ventricular cavity size and decreased systolic function are evidenced by increased residual/end-systolic volume (5). A reduced stroke volume is seen given the increased post-ejection residual volume and unchanged end-diastolic volume (6).

to IUGR, which may include other well-documented phenomena, such as the increased renin–angiotensin activity reported in human fetuses (Tsyvian *et al.* 2008). Unfortunately, given the lack of tissue at this stage of our study, we cannot yet comment on some physiologic responses that have been proposed to occur in IUGR, such as increased oxidative stress (Giussani *et al.* 2012; Kane *et al.* 2013; Nascimento *et al.* 2014; Vega *et al.* 2016; Itani *et al.* 2016) and endothelial and vascular dysfunction (Allison *et al.* 2016).

We acknowledge several limitations of this study. First, we should note that our evaluation is performed under anaesthesia, which is not without effects on cardiovascular function. In this study, we induce anaesthesia with ketamine, which is known for producing fewer effects on the cardiovascular system compared to other available agents, such as propofol or midazolam (Stowe *et al.* 1992). Similarly, of the many inhalational anaesthetics available, isoflurane has been shown to produce less impact to cardiovascular status (Kazama & Ikeda, 1988, Oguchi *et al.* 1995). Given that IUGR offspring are known to have increased sympathetic tone (Lee *et al.* 1998) and that ketamine has a sympathomimetic property that enhances the release of plasma catecholamine (Carruba *et al.* 1987), it is thought that the measured cardiac function decline being due to differing effects of anaesthesia between groups is unlikely. However, we cannot exclude the presence of paradoxical effect, and further studies may be warranted.

Secondly, we acknowledge the age disparity in our OLD animals. The OLD female baboons are several years younger than the OLD male baboons (13.6 ± 1.4 vs. 18.2 ± 2.6 years). While these age ranges both correlate to mid-to-late adulthood, this difference may impact some of our obtained measurements. Fortunately, when examining the parameters where sex differences were found (Table 5), no measurement stands out as likely to be strongly affected by this age difference in our OLD animals.

We should further note that by literature both sexes of the baboons have reached sexual maturity at age of 5.7. However, we did not measure sex hormones for confirmation. It is possible that delayed sexual maturation confounds our results on cardiac function, as it has been previously suggested that IUGR delays onset of puberty (Engelbregt *et al.* 2000). Nevertheless, we should further note that our findings of IUGR do not parallel that seen in paediatric patients. For example, a stable to minimally increased EF and mildly decreased normalized ESV are observed in normal human children (Poutanen *et al.* 2003) whereas we observed decreased EF and increased normalized ESV.

Also, the methodology used for determining ventricular volumes included papillary muscles as part of the lumen by convention. Although this approach affects the accuracy

of the measurement, it has been adopted as a convention to provide superior reproducibility (Papavassiliu *et al.* 2005). Lastly, the animals have metal identification tags implanted in their backs, which would sometimes cause artifacts that required interpolation from more basal or apical slices. Visually, this has not been a significant issue with performing measurements on the obtained images.

In this study, we have exploited the advantages of CMRI as a non-invasive method for determining cardiac function, resulting in clinically relevant parameters that are ready for translation. We have uncovered systolic dysfunction, diastolic derangement and morphological remodelling of the left ventricle in a baboon model in early adulthood. These findings suggest the previously reported cardiac abnormalities do indeed occur in primates and that at least some cardiac abnormalities of IUGR human neonates do persist into adulthood. Many of the IUGR findings parallel those of the OLD animals, but literature suggests divergent pathways governing those apparently similar changes. Although there are some inconsistencies between our findings and those of other animal models, we speculate that after accounting for species differences, varying effects of IUGR methods, timing of examination and normalization to BSA or MM, the non-uniformity in findings reported may simply reflect different aspects of the complicated and disrupted IUGR physiology. There are many advantages to our system in studying the IUGR, from the capability to examine physiology in prepubescent, newborn, or prenatal subjects *in vivo* that has been difficult by conventional means, to testing cardiovascular function under pharmaceutical stress (Vasu *et al.* 2015), or even testing other sequela of IUGR such as increased lipid deposition in the heart or other organs (McGavock *et al.* 2007). Magnetic resonance imaging and spectroscopy may represent invaluable assets that can supplement traditional analysis in obtaining a more holistic evaluation of primate physiology.

References

- Alexander BT, Dasinger JH & Intapad S (2015). Fetal programming and cardiovascular pathology. *Compr Physiol* **5**, 997–1025.
- Allison BJ, Kaandorp JJ, Kane AD, Camm EJ, Lusby C, Cross CM, Nevin-Dolan R, Thakor AS, Derks JB, Tarry-Adkins JL & Ozanne SE (2016). Divergence of mechanistic pathways mediating cardiovascular aging and developmental programming of cardiovascular disease. *FASEB J* **30**, 1968–1975.
- Barker DJ, Osmond C, Winter P, Margetts B & Simmonds SJ (1989). Weight in infancy and death from ischaemic heart disease. *Lancet* **334**, 577–580.
- Bjarnegård N, Morsing E, Cinthio M, Länne T & Brodzski J (2013). Cardiovascular function in adulthood following intrauterine growth restriction with abnormal fetal blood flow. *Ultrasound Obstet Gynecol* **41**, 177–184.
- Botting KJ, McMillen IC, Forbes H, Nyengaard JR & Morrison JL (2014). Chronic hypoxemia in late gestation decreases cardiomyocyte number but does not change expression of hypoxia-responsive genes. *J Am Heart Assoc* **3**, e000531.
- Brawley L, Itoh S, Torrens C, Barker A, Bertram C, Poston L & Hanson M (2003). Dietary protein restriction in pregnancy induces hypertension and vascular defects in rat male offspring. *Pediatr Res* **54**, 83–90.
- Bubb KJ, Cock ML, Black MJ, Dodic M, Boon W, Parkington HC, Harding R & Tare M (2007). Intrauterine growth restriction delays cardiomyocyte maturation and alters coronary artery function in the fetal sheep. *J Physiol* **578**, 871–881.
- Buller VG, Van Der Geest, RJ, Kool MD, Van Der Wall EE, De Roos A & Reiber JH (1997). Assessment of regional left ventricular wall parameters from short axis magnetic resonance imaging using a three-dimensional extension to the improved centerline method. *Invest Radiol* **32**, 529–539.
- Cai H, Yuan Z, Fei Q & Zhao J (2012). Investigation of thrombospondin-1 and transforming growth factor- β expression in the heart of aging mice. *Exp Ther Med* **3**, 433–436.
- Camm EJ, Hansell JA, Kane AD, Herrera EA, Lewis C, Wong S, Morrell NW & Giussani DA (2010). Partial contributions of developmental hypoxia and undernutrition to prenatal alterations in somatic growth and cardiovascular structure and function. *Am J Obstet Gynecol* **203**, 495.e24–495.e34.
- Carruba MO, Bondiolotti G, Picotti GB, Catteruccia N & Da Prada M (1987). Effects of diethyl ether, halothane, ketamine and urethane on sympathetic activity in the rat. *Eur J Pharmacol* **134**, 15–24.
- Cerqueira MD, Weissman NJ, Dilsizian V, Jacobs AK, Kaul S, Laskey WK, Pennell DJ, Rumberger JA, Ryan T, Verani MS & American Heart Association Writing Group on Myocardial Segmentation and Registration for Cardiac Imaging (2002). Standardized myocardial segmentation and nomenclature for tomographic imaging of the heart. A statement for healthcare professionals from the Cardiac Imaging Committee of the Council on Clinical Cardiology of the American Heart Association. *Circulation* **105**, 539–542.
- Cheema KK, Dent MR, Saini HK, Aroutiounova N & Tappia PS (2005). Prenatal exposure to maternal undernutrition induces adult cardiac dysfunction. *Br J Nutr* **93**, 471–477.
- Choi J, Li C, McDonald TJ, Comuzzie A, Mattern V & Nathanielsz PW (2011). Emergence of insulin resistance in juvenile baboon offspring of mothers exposed to moderate maternal nutrient reduction. *Am J Physiol Regul Integr Comp Physiol* **301**, R757–R762.
- Coleman-Jensen A, Gregory C & Singh A (2014). *Household Food Security in the United States in 2013*. USDA-ERS Economic Research Report. USDA Economic Research Service, Washington.
- Cox LA, Comuzzie AG, Havill LM, Karere GM, Spradling KD, Mahaney MC, Nathanielsz PW, Nicolella DP, Shade RE, Voruganti S & VandeBerg JL (2013). Baboons as a model to study genetics and epigenetics of human disease. *ILAR J* **54**, 106–121.

- Crispi F, Bijmens B, Figueras F, Bartrons J, Eixarch E, Le Noble F, Ahmed A & Gratacos E (2010). Fetal growth restriction results in remodeled and less efficient hearts in children. *Circulation* **121**, 2427–2436.
- Crispi F, Bijmens B, Sepulveda-Swatson E, Cruz-Lemini M, Rojas-Benavente J, Gonzalez-Tendero A, Garcia-Posada R, Rodriguez-Lopez M, Demicheva E, Sitges M & Gratacos E (2014). Postsystolic shortening by myocardial deformation imaging as a sign of cardiac adaptation to pressure overload in fetal growth restriction. *Circ Cardiovasc Imaging* **7**, 781–787.
- Engelbregt MJ, Houdijk ME, Popp-Snijders C & Delemarre-van de Waal HA (2000). The effects of intra-uterine growth retardation and postnatal undernutrition on onset of puberty in male and female rats. *Pediatr Res* **48**, 803–807.
- Fouzas S, Karatza AA, Davlouros PA, Chrysis D, Alexopoulos D, Mantagos S & Dimitriou G (2014). Neonatal cardiac dysfunction in intrauterine growth restriction. *Pediatr Res* **75**, 651–657.
- Fowden AL, Giussani DA & Forhead AJ (2006). Intrauterine programming of physiological systems: causes and consequences. *Physiology (Bethesda)* **21**, 29–37.
- Germans T, Götte MJ, Nijveldt R, Spreuwenberg MD, Beek AM, Bronzwaer JG, Visser CA, Paulus WJ & van Rossum AC (2007). Effects of aging on left atrioventricular coupling and left ventricular filling assessed using cardiac magnetic resonance imaging in healthy subjects. *Am J Cardiol* **100**, 122–127.
- Giussani DA, Camm EJ, Niu Y, Richter HG, Blanco CE, Gottschalk R, Blake EZ, Horder KA, Thakor AS, Hansell JA & Kane AD (2012). Developmental programming of cardiovascular dysfunction by prenatal hypoxia and oxidative stress. *PLoS One* **7**, e31017.
- Giussani D & Davidge S (2013). Developmental programming of cardiovascular disease by prenatal hypoxia. *J Dev Origins Health Dis* **4**, 328–337.
- Glassman DM, Coelho AM Jr, Carey KD & Bramblett CA (1984). Weight growth in savannah baboons: a longitudinal study from birth to adulthood. *Growth* **48**, 425–433.
- Gonzalez-Tendero A, Torre I, Garcia-Canadilla P, Crispi F, Garcia-Garcia F, Dopazo J, Bijmens B & Gratacos E (2013). Intrauterine growth restriction is associated with cardiac ultrastructural and gene expression changes related to the energetic metabolism in a rabbit model. *Am J Physiol Heart Circ Physiol* **305**, H1752–H1760.
- Hanson MA & Gluckman PD (2014). Early developmental conditioning of later health and disease: physiology or pathophysiology? *Physiol Rev* **94**, 1027–1076.
- Harvey TJ, Murphy RM, Morrison JL & Posterino GS (2015). Maternal nutrient restriction alters Ca²⁺ handling properties and contractile function of isolated left ventricle bundles in male but not female juvenile rats. *PLoS One* **10**, e0138388.
- Hees PS, Fleg JL, Lakatta EG & Shapiro EP (2002). Left ventricular remodeling with age in normal men versus women: novel insights using three-dimensional magnetic resonance imaging. *Am J Cardiol* **90**, 1231–1236.
- Iruetagoiena JI, Gonzalez-Tendero A, Garcia-Canadilla P, Amat-Roldan I, Torre I, Nadal A, Crispi F & Gratacos E (2014). Cardiac dysfunction is associated with altered sarcomere ultrastructure in intrauterine growth restriction. *Am J Obstet Gynecol* **210**, 550.e1–550.e7.
- Itani N, Skeffington KL, Beck C, Niu Y & Giussani DA (2016). Melatonin rescues cardiovascular dysfunction during hypoxic development in the chick embryo. *J Pineal Res* **60**, 16–26.
- Jones A, Beda A, Osmond C, Godfrey KM, Simpson DM & Phillips DI (2008). Sex-specific programming of cardiovascular physiology in children. *Eur Heart J* **29**, 2164–2170.
- Kane AD, Herrera EA, Camm EJ & Giussani DA (2013). Vitamin C prevents intrauterine programming of in vivo cardiovascular dysfunction in the rat. *Circ J* **77**, 2604–2611.
- Kawamura M, Itoh H, Yura S, Mogami H, Suga SI, Makino H, Miyamoto Y, Yoshimasa Y, Sagawa N & Fujii S (2007). Undernutrition in utero augments systolic blood pressure and cardiac remodeling in adult mouse offspring: possible involvement of local cardiac angiotensin system in developmental origins of cardiovascular disease. *Endocrinology* **148**, 1218–1225.
- Kazama T & Ikeda K (1988). The comparative cardiovascular effects of sevoflurane with halothane and isoflurane. *J Anesth* **2**, 63–68.
- Keenan K, Bartlett TQ, Nijland M, Rodriguez JS, Nathanielsz PW & Zurcher NR (2013). Poor nutrition during pregnancy and lactation negatively affects neurodevelopment of the offspring: evidence from a translational primate model. *Am J Clin Nutr* **98**, 396–402.
- Kitzman DW, Little WC, Brubaker PH, Anderson RT, Hundley WG, Marburger CT, Brosnihan B, Morgan TM & Stewart KP (2002). Pathophysiological characterization of isolated diastolic heart failure in comparison to systolic heart failure. *JAMA* **288**, 2144–2150.
- Lambie-Mumford H & Dowler E (2014). Rising use of “food aid” in the United Kingdom. *Br Food J* **116**, 1418–1425.
- Langley-Evans SC (2013). Fetal programming of CVD and renal disease: animal models and mechanistic considerations. *Proc Nutr Soc* **72**, 317–325.
- Langley-Evans SC (2015). Nutrition in early life and the programming of adult disease: a review. *J Hum Nutr Diet* **28** (Suppl 1), 1–14.
- Lee J, Park K, Hwang J, Park M & Yum M (1998). Chaotic and periodic heart rate dynamics in uncomplicated intrauterine growth restricted fetuses. *Early Hum Dev* **53**, 121–128.
- Leigh SR (2009). Growth and development of baboons. In *The Baboon in Biomedical Research*, ed. VandeBerg JL, Williams-Blangero S & Tardiff SD, pp. 57–88. Springer, New York.
- Li C, Ramahi E, Nijland MJ, Choi J, Myers DA, Nathanielsz PW & McDonald TJ (2013a). Up-regulation of the fetal baboon hypothalamo-pituitary-adrenal axis in intrauterine growth restriction: coincidence with hypothalamic glucocorticoid receptor insensitivity and leptin receptor down-regulation. *Endocrinology* **154**, 2365–2373.

- Li C, McDonald TJ, Wu G, Nijland MJ & Nathanielsz PW (2013b). Intrauterine growth restriction alters term fetal baboon hypothalamic appetitive peptide balance. *J Endocrinol* **217**, 275–282.
- McGavock JM, Lingvay I, Zib I, Tillery T, Salas N, Unger R, Levine BD, Raskin P, Victor RG & Szczepaniak LS (2007). Cardiac steatosis in diabetes mellitus: A ^1H -magnetic resonance spectroscopy study. *Circulation* **116**, 1170–1175.
- Maceira A, Prasad S, Khan M & Pennell D (2006a). Normalized left ventricular systolic and diastolic function by steady state free precession cardiovascular magnetic resonance. *J Cardiovasc Magn Reson* **8**, 417–426.
- Maceira AM, Prasad SK, Khan M & Pennell DJ (2006b). Reference right ventricular systolic and diastolic function normalized to age, gender and body surface area from steady-state free precession cardiovascular magnetic resonance. *Eur Heart J* **27**, 2879–2888.
- Maloyan A, Muralimanoharan S, Nijland M & Nathanielsz PW (2014). Sexual dimorphism in cardiac response to intrauterine growth restriction (IUGR). *Circulation* **130**, A15515.
- Mannaerts HF, van der Heide JA, Kamp O, Stoel MG, Twisk J & Visser CA (2004). Early identification of left ventricular remodelling after myocardial infarction, assessed by transthoracic 3D echocardiography. *Eur Heart J* **25**, 680–687.
- Mastorci F, Vicentini M, Viltart O, Manghi M, Graiani G, Quaini F, Meerlo P, Nalivaiko E, Maccari S & Sgoifo A (2009). Long-term effects of prenatal stress: changes in adult cardiovascular regulation and sensitivity to stress. *Neurosci Biobehav Rev* **33**, 191–203.
- Menendez-Castro C, Toka O, Fahlbusch F, Cordasic N, Wachtveitl R, Hilgers KF, Rascher W & Hartner A (2014). Impaired myocardial performance in a normotensive rat model of intrauterine growth restriction. *Pediatr Res* **75**, 697–706.
- Miyague N, Ghidini A, Fromberg R & Miyague L (1997). Alterations in ventricular filling in small-for-gestational-age fetuses. *Fetal Diagn Ther* **12**, 332–335.
- Nascimento L, Freitas CM, Silva-Filho R, Leite AC, Silva AB, da Silva AI, Ferreira DS, Pedroza AA, Maia MB, Fernandes MP & Lagranha C (2014). The effect of maternal low-protein diet on the heart of adult offspring: role of mitochondria and oxidative stress. *Appl Physiol Nutr Metab* **39**, 880–887.
- Nathanielsz PW, Nijland MJ, Nevill CH, Jenkins SL, Hubbard GB, McDonald TJ & Schlabritz-Loutsevitch NE (2009). Baboon model for the study of nutritional influences on pregnancy. In *The Baboon in Biomedical Research*, ed. VandeBerg JL, Williams-Blangero S & Tardiff SD, pp. 237–253. Springer, New York.
- Oguchi T, Kashimoto S, Yamaguchi T, Nakamura T & Kumazawa T (1995). Comparative effects of halothane, enflurane, isoflurane and sevoflurane on function and metabolism in the ischaemic rat heart. *Br J Anaesth* **74**, 569–575.
- Papavassiliu T, Kühl HP, Schröder M, Süselbeck T, Bondarenko O, Böhm CK, Beek A, Hofman MM & van Rossum AC (2005). Effect of endocardial trabeculae on left ventricular measurements and measurement reproducibility at cardiovascular MR imaging. *Radiology* **236**, 57–64.
- Peshock RM, Rokey R, Malloy CM, McNamee P, Buja LM, Parkey RW & Willerson JT (1989). Assessment of myocardial systolic wall thickening using nuclear magnetic resonance imaging. *J Am Coll Cardiol* **14**, 653–659.
- Pfeiffer S, Ritter T & Oestreicher E (2015). Food insecurity in German households: qualitative and quantitative data on coping, poverty consumerism and alimentary participation. *Soc Policy Soc* **14**, 483–495.
- Poutanen T, Jokinen E, Sairanen H & Tikanoja T (2003). Left atrial and left ventricular function in healthy children and young adults assessed by three dimensional echocardiography. *Heart* **89**, 544–549.
- R Core Team (2013). *R: A Language and Environment for Statistical Computing*. <http://www.R-project.org/>. R Foundation for Statistical Computing, Vienna, Austria.
- Rich-Edwards JW, Stampfer MJ, Manson JE, Rosner B, Hankinson SE, Colditz GA, Willett WC & Hennekens CH (1997). Birth weight and risk of cardiovascular disease in a cohort of women followed up since 1976. *BMJ* **315**, 396–400.
- Rizzo G, Capponi A, Rinaldo D, Arduini D & Romanini C (1995). Ventricular ejection force in growth-retarded fetuses. *Ultrasound Obstet Gynecol* **5**, 247–255.
- Rodríguez-González GL, Reyes-Castro LA, Vega CC, Boeck L, Ibáñez C, Nathanielsz PW, Larrea F & Zambrano E (2014). Accelerated aging of reproductive capacity in male rat offspring of protein-restricted mothers is associated with increased testicular and sperm oxidative stress. *Age* **36**, 1–12.
- Rogers J, Mahaney MC, Witte SM, Nair S, Newman D, Wedel S, Rodriguez LA, Rice KS, Slifer SH & Perelygin A (2000). A genetic linkage map of the baboon (*Papio hamadryas*) genome based on human microsatellite polymorphisms. *Genomics* **67**, 237–247.
- Rueda-Clausen CF, Morton JS, Lopaschuk GD & Davidge ST (2010). Long-term effects of intrauterine growth restriction on cardiac metabolism and susceptibility to ischaemia/reperfusion. *Cardiovasc Res* **90**, 285–294.
- Schlabritz-Loutsevitch NE, Howell K, Rice K, Glover EJ, Nevill CH, Jenkins SL, Bill Cummins L, Frost PA, McDonald TJ & Nathanielsz PW (2004). Development of a system for individual feeding of baboons maintained in an outdoor group social environment. *J Med Primatol* **33**, 117–126.
- Shively CA & Clarkson TB (2009). The unique value of primate models in translational research. *Am J Primatol* **71**, 715–721.
- Stacy V, De Matteo R, Brew N, Sozo F, Probyn ME, Harding R & Black MJ (2009). The influence of naturally occurring differences in birthweight on ventricular cardiomyocyte number in sheep. *Anat Rec* **292**, 29–37.
- Stowe DF, Bosnjak ZJ & Kampine JP (1992). Comparison of etomidate, ketamine, midazolam, propofol, and thiopental on function and metabolism of isolated hearts. *Anesth Analg* **74**, 547–558.
- Sun C, Burgner DP, Ponsonby A, Saffery R, Huang R, Vuillermin PJ, Cheung M & Craig JM (2013). Effects of early-life environment and epigenetics on cardiovascular disease risk in children: highlighting the role of twin studies. *Pediatr Res* **73**, 523–530.
- Tarrade A, Panchenko P, Junien C & Gabory A (2015). Placental contribution to nutritional programming of health and diseases: epigenetics and sexual dimorphism. *J Exp Biol* **218**, 50–58.

- Tarry-Adkins JL & Ozanne SE (2014). The impact of early nutrition on the ageing trajectory. *Proc Nutr Soc* **73**, 289–301.
- Taylor P, Samuelsson A & Poston L (2014). Maternal obesity and the developmental programming of hypertension: a role for leptin. *Acta Physiol (Oxf)* **210**, 508–523.
- Thiele H, Paetsch I, Schnackenburg B, Bornstedt A, Grebe O, Wellnhofer E, Schuler G, Fleck E & Nagel E (2002). Improved accuracy of quantitative assessment of left ventricular volume and ejection fraction by geometric models with steady-state free precession. *J Cardiovasc Magn Reson* **4**, 327–339.
- Thornburg K (2015). The programming of cardiovascular disease. *J Dev Origin Health Dis* **6**, 366–376.
- Tsyvian PB, Markova TV, Mikhailova SV, Hop WC & Wladimiroff JW (2008). Left ventricular isovolumic relaxation and renin-angiotensin system in the growth restricted fetus. *Euro J Obst Gyn Reprod Biol* **140**, 33–37.
- Vasu S, Little WC, Morgan TM, Stacey RB, Ntim WO, Hamilton C, Thohan V, Chiles C & Hundley WG (2015). Mechanism of decreased sensitivity of dobutamine associated left ventricular wall motion analyses for appreciating inducible ischemia in older adults. *J Cardiovasc Magn Reson* **17**, 26.
- Vega CC, Reyes-Castro LA, Rodríguez-González GL, Bautista CJ, Vázquez-Martínez M, Larrea F, Chamorro-Cevallos GA, Nathanielsz PW & Zambrano E (2016). Resveratrol partially prevents oxidative stress and metabolic dysfunction in pregnant rats fed a low protein diet and their offspring. *J Physiol* **594**, 1483–1499.
- Ward AM, Moore VM, Steptoe A, Cockington RA, Robinson JS & Phillips DI (2004). Size at birth and cardiovascular responses to psychological stressors: evidence for prenatal programming in women. *J Hypertens* **22**, 2295–2301.
- Weber KT, Brilla CG & Janicki JS (1993). Myocardial fibrosis: functional significance and regulatory factors. *Cardiovasc Res* **27**, 341–348.
- Xu Y, Williams SJ, O'Brien D & Davidge ST (2006). Hypoxia or nutrient restriction during pregnancy in rats leads to progressive cardiac remodeling and impairs postischemic recovery in adult male offspring. *FASEB J* **20**, 1251–1253.
- Yeung EH, Robledo C, Boghossian N, Zhang C & Mendola P (2014). Developmental origins of cardiovascular disease. *Curr Epidemiol Rep* **1**, 9–16.
- Zambrano E & Nathanielsz PW (2013). Mechanisms by which maternal obesity programs offspring for obesity: evidence from animal studies. *Nutr Rev* **71** (Suppl 1), S42–S54.
- Zambrano E, Reyes-Castro LA & Nathanielsz PW (2015). Aging, glucocorticoids and developmental programming. *Age* **37**, 9774.
- Zohdi V, Black MJ & Pearson JT (2011). Elevated vascular resistance and afterload reduce the cardiac output response to dobutamine in early growth-restricted rats in adulthood. *Br J Nutr* **106**, 1374–1382.
- Zohdi V, Lim K, Pearson JT & Black MJ (2014). Developmental programming of cardiovascular disease following intrauterine growth restriction: findings utilising a rat model of maternal protein restriction. *Nutrients* **7**, 119–152.
- Zohdi V, Wood BR, Pearson JT, Bamberg KR & Black MJ (2013). Evidence of altered biochemical composition in the hearts of adult intrauterine growth-restricted rats. *Euro J Nutr* **52**, 749–758.

Additional information

Competing interests

None of the authors has any conflicts of interest to disclose.

Author contributions

A.H.K. participated in the design of the work, acquisition, analysis and interpretation of data, and drafting the manuscript and revising it critically for important intellectual content. C.L. participated in the design of the work, data acquisition and revising the manuscript critically for important intellectual content. J.L. participated in the design of the work, data acquisition and revising the manuscript critically for important intellectual content. H.F.H. participated in the design of the work, data acquisition and analysis, and revising the manuscript critically for important intellectual content. P.W.N. participated in the conception and design of the work, interpretation of data and in revising the manuscript critically for important intellectual content. G.D.C. participated in the conception and design of the work, data analysis, interpretation of data and writing and revising the manuscript. All authors approved the final version of the manuscript, agree to be accountable for all aspects of the work in ensuring that questions related to the accuracy or integrity of any part of the work are appropriately investigated and resolved and all persons designated as authors qualify for authorship, and all those who qualify for authorship are listed.

Funding

This work was supported by the National Institutes of Health 5P01HD021350 and 5R24OD011183 (P.W.N.), 5K25DK089012 (G.D.C.) and 1R25EB016631 (A.H.K.). NIH grant OD P51 OD011133 was from the Office of Research Infrastructure Programs/Office of the Director. This work was also supported in part by funding from the EU FP 7/HEALTH/GA No.: 279281: BrainAge - Impact of Prenatal Stress on BRAINAGEing.

Acknowledgements

The authors thank Dr Robert Lanford and the Southwest National Primate Center for their ongoing support of the baboon research program described in this article. The authors also acknowledge the technical support of Steven Rios and Susan Jenkins, as well as the administrative support of Karen Moore.